Orbital
The electronic journal of chemistry

the electronic journal of chemistry

Full Paper | http://dx.doi.org/10.17807/orbital.v13i2.1446

TiO_2 Synthesis by Pechini Method and Application in Dye-Sensitized Solar Cells

Gideã Taques Tractz* [a], Bianca Vanjura Dias [a], Guilherme Arielo Rodrigues Maia [b], and Paulo Rogério Pinto Rodrigues [a]

Dye-sensitized solar cells (DSSC) are devices to solar energy conversion, which present low production costs and high photoelectrochemical stability. The aim of this study was to investigate the synthesis of TiO_2 by Pechini methodology, using $C_{12}H_{28}O_4Ti$ and $TiCl_3$ as precursors, and their application in solar cell sensitized by N719 dye. The characterization techniques employed were Scanning Electron Microscopy (SEM), UV-VIS Spectroscopy, X-ray diffraction (XRD), photochronoamperometry, j-V Curves and EIS plots. The results demonstrated a high crystallinity and surface area to particles obtained with $C_{12}H_{28}O_4Ti$ as precursor. The highest photoconversion energy efficiency reached was to TiO_2 using $C_{12}H_{28}O_4Ti$ with PCE= 4.17±0.13% with photoelectrochemical parameters of j_{sc}= 5.53 ±0.08, V_{oc}= 0.78±0.07 FF=0.58±0.05 and less resistive to charge transport with τ_e= 53 ms.

Graphical abstract

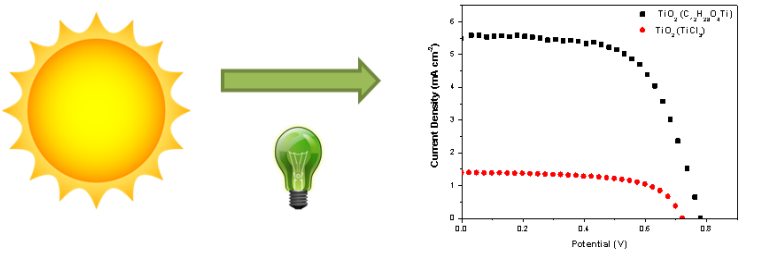

TiO_2 Precursor	j_{sc} /mA cm^{-2}	V_{oc} /V	FF	PCE/%
TiO_2 ($C_{12}H_{28}O_4Ti$)	5.53±0.08	0.78±0.07	0.58±0.05	4.17±0.13
TiO_2 ($TiCl_3$)	1.42±0.03	0.72±0.01	0.65±0.02	1.11±0.04

Keywords

Gratzel cells
Pechini
PV cells

Article history

Received 12 November 2019
Revised 10 March 2021
Accepted 31 March 2021
Available online 08 June 2021

Handling Editor: Sergio R. Lázaro

1. Introduction

The search for new energy resources will take the first place in worldwide problems for 2050, in front of polemics issues like poverty, terrorism and water, as shown by Smalley in Materials Matter Journal [1]. This is estimated, due to the high demand required to supply about 9 billion people present in the whole world. However, the great questions are: Do we have enough energy? Are fossil fuels the solution for energy supply? How climate changes affect the search for new energy resources?

Renewable alternatives that can be applied in energy conversion are the keys to a sustainable future. At this point, solar cells are free pollution devices and it has some advantages as easy installation, maintenance and does not require high investments in transmission lines [2]. On the other hand, the silicon-based solar cells which are the most used system, present a high production cost due to the

[a] Universidade Estadual do Centro, Campus Cedeteg, Departamento de Química, Rua Simeão Varela de Sá, 03, Vila Carli, Guarapuava-PR, Brazil. [b] Universidade Estadual de Londrina, Rodovia Celso García Cid- Pr 445, Km 380, Londrina-PR Brazil. *Corresponding author. E-mail: **gide.tractz@hotmail.com**

Czochralski method of crystal growth, leading the research of new photovoltaic systems with reduced costs [3].

The third generation of solar cells has attracted much attention, since 1991, when O'Regan and Gratzel in the Laboratory of Photonics and Interfaces at École Polytechnique Federale of Lausanne, Switzerland, discovered that a sensitized mesoporous semiconductor oxide can generate charges when exposed to light [4, 5]. This was the beginning of a new form of energy conversion, which is one of the greatest challenges in the century.

Dye-sensitized solar cells (DSSC) are solar devices that consist of an organic photosensitive dye, anchored on top of a semiconductor oxide [6]. When the cell is irradiated by sunlight, the electrons from HOMO state are injected to dye LUMO state, which are injected into the conduction band of semiconductor oxide, generating a current flow [7].TiO_2 is the most used scaffold semiconductor material for these systems, due to some characteristics such as the position of valence and conduction band, high photochemistry stability and low production synthesis [8]. On the other hand, this oxide presents a complex synthetic route to suitable particle production, usually always requiring high-pressure reactors [8]. Guimarães and co-workers demonstrated the TiO_2 synthesis using a Teflon autoclave at 230 ºC for 12 hours with a pre-treatment at 80 ºC for 8 hours using the hydrothermal method [9]. Other routes, as co-precipitation, sol-gel, combustion, etc are being applied to particle preparation and have been presented excellent results [10–13].

Pechini synthesis, derivated from the sol-gel method, has attracted a lot of attention from researches, due to the possibility to work with different temperatures and proportions and to control stoichiometry and size for nanometric particle production [10]. This process consists of the use of carboxylic acid to form a chelate, which with an alcohol presence, via condensation, produces esters groups. With high temperature, the organic phase is eliminated, and the oxide is obtained as demonstrated by Dimesso [14].

This work aims to study the TiO_2 synthesis by the Pechini methodology, using titanium trichloride ($TiCl_3$) and titanium isopropoxide ($C_{12}H_{28}O_4Ti$) as precursors and their application in dye-sensitized solar cells (DSSC).

2. Results and Discussion

Figure 1 presents the X-Ray Diffraction (XRD) for particles synthesized, to verify the obtained phase to particles produced.

Both particles presented correspondent peaks, characteristic to TiO_2 in anatase form (Figure 1) by comparison with the crystallographic record PDF 71-1166 using EVA® software. The cataloging of Titanium dioxide presents three crystallographic forms: rutile, anatase and brookite [8]. However, anatase is recommended to solar cell production, due to the higher surface area per volume and crystal density, relative to other phases, forming as a "trap" for electrons, increasing their application as electron scaffold, as related by Muniz et. al. [15].

On the other hand, it is noted narrow peaks, especially the (101) crystallographic plane for the TiO_2 synthesized by $C_{12}H_{28}O_4Ti$ as a precursor. Dadkah et. al related that anatase phase presents a low electron recombination rate of electron/oxidized electrolyte, caused by the low temperatures of thermic treatment [16]. This suggests that cell with TiO_2 produced from $TiCl_3$ precursor present lower electron lifetime in solar cells, due to the lower oxides crystallization, however, this hypothesis can only be confirmed by the frequency measurements like EIS plots.

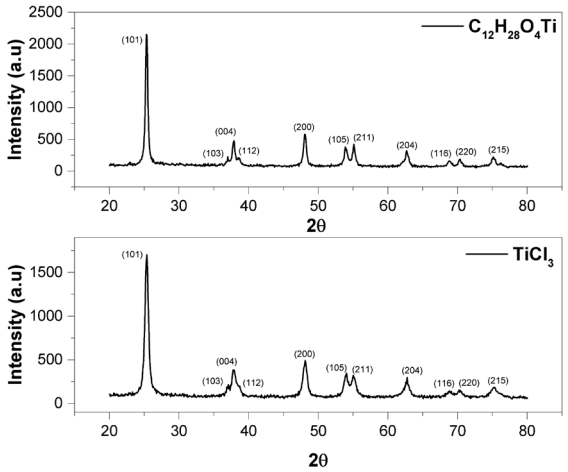

Fig. 1. XRD obtained to TiO_2 particles using $C_{12}H_{28}O_4Ti$ and $TiCl_3$ as precursors by the Pechini method.

Figure 2 shows the SEM images for TiO_2 particles synthesized using $C_{12}H_{28}O_4Ti$ and $TiCl_3$ in Pechini method.

The TiO_2 particles presented agglomerates with irregular morphology for both precursors. Maia related that the irregular morphology is efficiently for dye solar cells preparation, due to the available area for dye adsorption [17]. When material presents a large area, it presents some significant spaces to dye coordination, leading to better electrons inject under solar illumination and higher photocurrent values.

In literature, is related that Cl^- ions are able to bond in the particles, generating higher agglomerate rates that are not beneficial to particles to solar application, due to the low surface area [18, 19]. To evaluate this suggestion of low surface area to TiO_2 synthesized by $TiCl_3$ precursor, the amounts of adsorbed dye molecules were determined by UV-VIS analysis of a standard concentration vs absorption plots, after desorbing the dye from the oxide, using 0.1 mol L^{-1} of NaOH solution [20]. The results are shown in Table 1.

Table 1. N719 concentration obtained for studied cells, by spectrophotometrically analyze.

Particles	Concentration (mmol L^{-1} cm^{-2})
TiO_2 ($C_{12}H_{28}O_4Ti$)	0.046
TiO_2 ($TiCl_3$)	0.010

y= 0.00632+ 12.7608 x; r= 0.9997

It is noted, that TiO_2 synthesized with $C_{12}H_{28}O_4Ti$ presented a higher surface area, due to the higher amounts of dye adsorbed in the oxide. It can be suggested to the surface area of the film was increased, which may generate cells with better photovoltaic parameters [5]. To confirm this point, electrochemical measurements were performed and the photochronoamperometry curves are shown in Figure 3 to cells analyzed.

The cell was put in dark condition and after in light condition, to verify the photochronoamperometric curves, which provide analysis of stability and current density for solar cells.

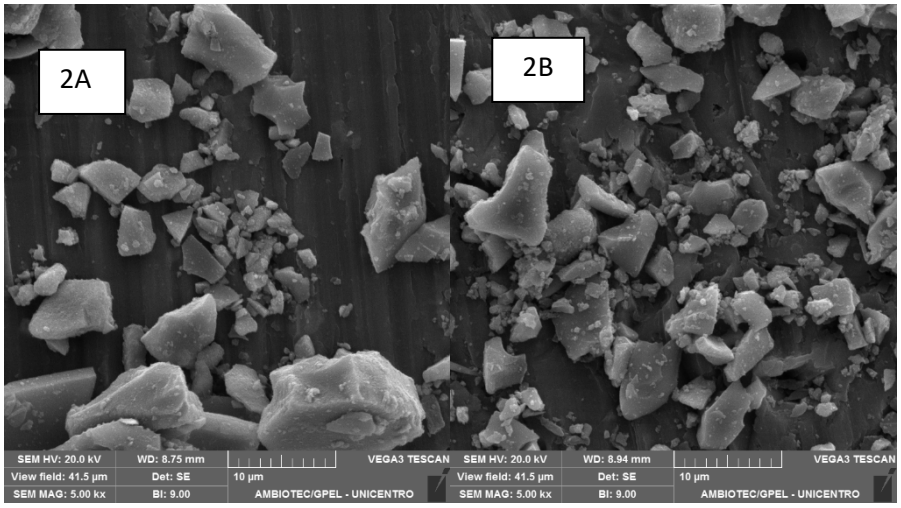

Fig. 2.SEM images of the TiO_2 particles synthesized by Pechini route using $C_{12}H_{28}O_4Ti$ in 2A and $TiCl_3$ in 2B as precursors.

All produced DSSC are photosensitive since once there was solar incidence light, the cells showed an instantaneous increase in the photocurrent as depicted in Figure 3 [21]. This capability of instantaneous injection, show fast interfacial reactions, necessary phenomenon to efficient solar cells [22]. It is also noted, electrolyte diffusional process in cell with TiO_2 ($C_{12}H_{28}O_4Ti$), until reach an equilibrium, however, it was not seen any degradation sign in the time performed [7].

Cells produced with TiO_2 from $C_{12}H_{28}O_4Ti$ presented better photocurrent, close to 6 mA cm^{-2}, due to the large surface area as demonstrated in Table 1. The use of TiO_2 from $TiCl_3$ precursor generates a cell with a low photocurrent (1.5 mA cm^{-2}), and these results must influence the harvesting light capability of the cells, as shown by IPCE spectra in Figure 4.

The IPCE spectra provide a detailed analysis of conversion efficiency in photon incident by electron, in different wavelengths [23]. In addition to previous measurements, IPCE spectrum showed better energy conversion to cell produced using $C_{12}H_{28}O_4Ti$ as precursor. It reached an IPCE maximum of 39 % in a region of 517 nm, and it indicates a high generation of charge carriers due the better surface area when compared to DSSC with TiO_2 from $TiCl_3$ precursor [24].

This photosensitive region showed in IPCE spectra for both cells, is characteristic from N719 dye used, since both cells presented the same regions of electrons absorption, however, with different IPCE values due to TiO_2 particles characteristics. In literature, it is related to similar IPCE ranges for using the N719 dye [9].

The j-V curves were performed, and the results are shown in Figure 5 and Table 2.

The photovoltaic parameters extracted from the j-V curves showed higher photoconversion energy efficiency (4.17% ± 0.13) to the TiO_2 solar cell produced with $C_{12}H_{28}O_4Ti$ as the precursor. According to Thavasi et al. [25], the photocurrent is associated with electron injection mechanism, the charge transport carriers and the dye adsorption in TiO_2 surface. The results obtained in this measurement is according to previously performed analyzes since it was verified a higher surface area for these particles. DSSC that can generate high photocurrent, produces better efficiencies since *j* is proportional to PCE value [22].

Table 2. Photovoltaic parameters extract to current curves vs potential.

TiO_2 Precursor	j_{sc} /mA cm^{-2}	V_{oc} /V	FF	PCE/%
TiO_2 ($C_{12}H_{28}O_4Ti$)	5.53±0.08	0.78±0.07	0.58±0.05	4.17±0.13
TiO_2 ($TiCl_3$)	1.42±0.03	0.72±0.01	0.65±0.02	1.11±0.04

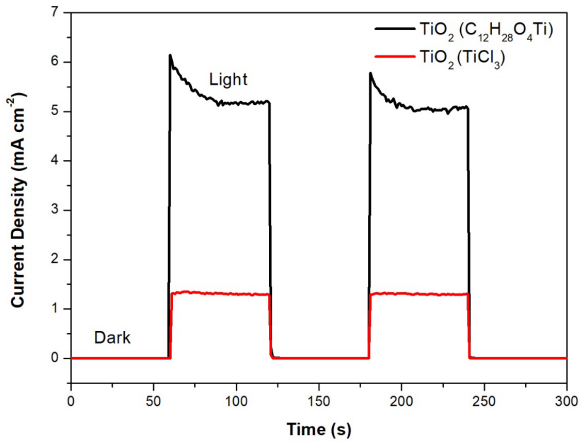

Fig. 3. Photocronoamperometry curves to DSSCs with TiO_2 synthesized with $C_{12}H_{28}O_4Ti$ and $TiCl_3$ under solar illumination of 60 mW cm^{-2}.

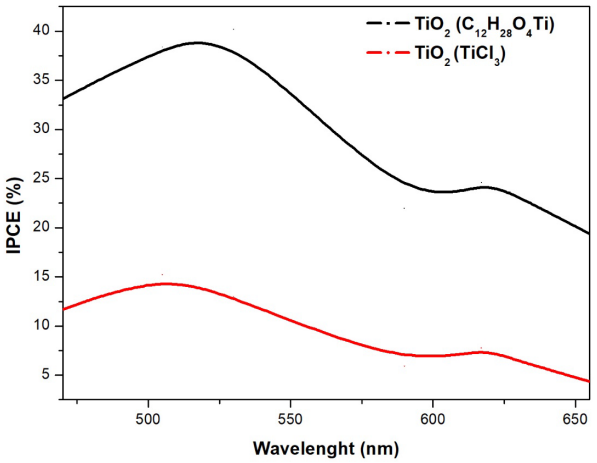

Fig. 4. IPCE spectra of DSSC with TiO_2 synthesized with $C_{12}H_{28}O_4Ti$ and $TiCl_3$ in a range of 470 nm to 655 nm.

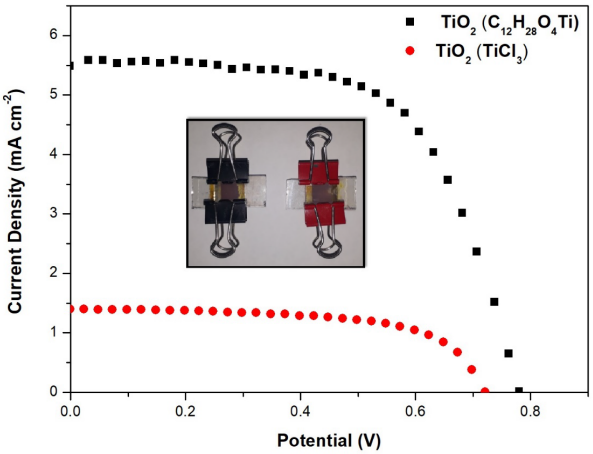

Fig. 5. j-V Curves to solar cells with TiO_2 synthesized with $C_{12}H_{28}O_4Ti$ and $TiCl_3$ under solar illumination of 60 mW cm^{-2}.

The FF values, which is an ideal factor from 0 to 1, being 1 the ideal cell with high PCE, the results obtained were promissory for both cells, however, the less diffusional process in particles, as seen in photochonoamperometry measurement, produced a cell with higher FF to the use of TiO_2 ($TiCl_3$) particles [23]. On the other hand, this result can be improved, due to in the literature values around 0.7 can easily be found by the change of film thickness and structure modification [26, 27].

V_{oc} is related to the difference between the Fermi Level of metal oxide and the Nernst potential of the electrolyte redox couple [28]. Viomar et al. demonstrated that higher V_{oc} values indicate that recombination processes were minimized, and low potential indicates pronunciation electron recombination [26]. The recombination process can be explained by back-electron-transfer reaction from the conduction band of semiconductor to the oxidized sensitizer or oxidized species of, generating heat losses [29]. For the DSSCs analyzed, TiO_2 produced by $TiCl_3$ as a precursor, showed low V_{oc} confirming for this system that the recombination reaction is more pronounced. The IES measurement was performed and the results are available in Figure 6.

It is noted in Figure 6, the formation of three capacitive arcs to TiO_2 from $C_{12}H_{28}O_4Ti$ precursor. This EIS behavior is according to ideal DSSC systems since the first capacitive arc in higher frequencies indicates the charge transfer in counter electrode, intermediary frequency the electron transport and diffusion in TiO_2 conduction band and in lower frequencies the electrolyte diffusion [9, 30]. In the case of cells tested, the use of $TiCl_3$ showed only one arc, indicating enhanced recombination reaction is able to suppress the visualization of charge transfer in cathode and electrolyte diffusion.

Higher resistances show the difficulty of electron transport, decreasing the j_{sc} and V_{oc} parameters as shown in j-V curves. It is possible as demonstrated by Bisquert [31, 32] use the impedance with three capacitive arcs to find the electron lifetime (the relaxation time that for solar cells is equivalent to electron recombination, present in TiO_2 conduction band to oxidized electrolyte) using the model of Figure 7 [33]. The τ_e for DSSC with $TiCl_3$ was not calculated, since there is no EIS adjustment model for DSSC with only one capacitive arc.

The values obtained to the cell which used $C_{12}H_{28}O_4Ti$ were 1.54 mF to chemical capacitance (Cμ), and 34.41 to recombination resistance (R_{rec}). The electron lifetime (τ_e) was calculated by the product of Cμ and R_{rec}, and was obtained τ_e = 53 ms, equivalent results to TiO_2 commercial [9, 29].

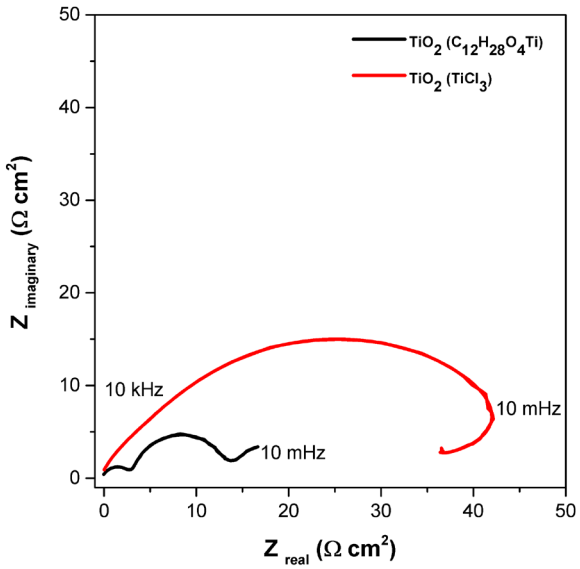

Fig. 6. Nyquist plot to DSSC produced with particles synthesized from $C_{12}H_{28}O_4Ti$ and $TiCl_3$ as precursors.

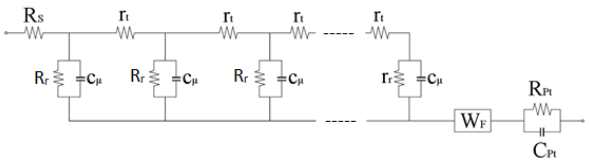

Figure 7. Adjustment model for DSSC with three capacitive arcs.

3. Material and Methods

TiO_2 oxide was synthesized adding 50 mL of citric acid solution (1 mol L^{-1}) and stirring at 70 °C. After, the metallic precursor was added in 2:1 molar proportion (citric acid: metallic cation) with 34 mL of ethylene glycol, under stirring until 90 °C for 30 minutes [10]. The resin was put in a mortar and calcinated until 400 °C for 2.5 h to puff deagglomeration [10]. Then, it was thermally treated at 500 °C for 2.5 h. The powder obtained was macerated for 5 min, to deagglomeration.

TiO_2 photoanode was prepared with 3 g of produced oxide, adding 0.1 mL of acetylacetone, 1 mL polyethylene glycol, 0.1 mL Triton X and 4 mL of deionized water [34, 35]. The produced paste was coated by Doctor Blading method in a transport conductor oxide glass (TCO) of FTO (fluorine-doped tin oxide ~7 Ω sq^{-1}). After deposition, the substrates were calcinated at 450 °C for 30 min.

To sensitize, the semiconductor material was immersed in dye solution at 2.5. 10^{-4} mol L^{-1} of N719 (di-tetrabutylammonium *cis*- bis (2,2'-bipyridyl – 4,4'-dicarboxylate) ruthenium (II)) in ethanol solution for 12 h [6]. The cells were assembled in the sandwich format of anode and cathode, with an active area of 0.2 cm^2, using electrodeposited platinum by cyclic voltammetry as cathode and $3I^-/I_3^-$ as electrolyte [36].

The oxides morphologies were evaluated by Scanning

Electron Microscope (SEM) images (Model Tescan® Vega 3) with an energy of 20 kV. Powder X-ray diffraction was recorded in a Bruker XRD D2 Phaser instrument, using CuKa radiation source with a wavelength of 0.15406 nm operated at 30 kV and 10 mA. The UV VIS analyzes were performed in a Gehaka 320 instrument, at a wavelength of 530 nm at 25 ºC.

The electrochemical measurements were obtained under illumination with an AM 1.5G using an intensity of 60 mW cm^{-2} (Model Zhenium Zhaner® with a solar simulator LOT ORIEL LS0106) at 25 °C. The counter electrode was short-circuited with a reference electrode and put in the platinum plate, and the working electrode was taken in photoanode plate. The photoconversion energy efficiency (PCE) was calculated as follows [22, 37]:

$$PCE = \frac{j_{sc} V_{oc} FF}{P} \text{ (Equation 1)}$$

j_{sc} is the short circuit current, P_{in} power of the incidence light, V_{OC} the open circuit potential, and FF the fill factor of the cell, defined as the ratio of the maximum power output from a DSSC to produce the j_{sc} and V_{oc} [6].

The IPCE spectra were measured by irradiating the device in wavelength of 470 nm, 505 nm, 530 nm 590 nm, 617 nm, 627 nm, and 625 nm, measuring the current/voltage output in an autolab potentiostat model PGSTAT303N from Metrohm®. The IPCE values were obtained using Equation 2, where λ is wavelength of incident light.

$$IPCE = \frac{J_{cc}(\lambda)[Acm^{-2}]}{\lambda(nm)P \quad (\lambda)[Wcm^{-2}]} \text{ (Equation 2)}$$

Electrochemical Impedance Spectroscopy (EIS) were recorded in the frequency range between 10 mHz and 10 KHz, an irradiance of 60 mW cm^{-2}, under standard illumination of AM 1.5 and perturbation in V_{oc} of 10 mV

4. Conclusions

The use of $C_{12}H_{28}O_4Ti$ as a precursor to producing TiO_2 particles generates a higher crystallinity and surface area oxide when compared to the use of $TiCl_3$ using Pechini Method. These characteristics were fundamental to production of a cell with enhanced photoconversion energy efficiency.

All the devices studied were photosensitive as shown in photochronoamperometric curves. However, the use of TiO_2 particles synthesized with $C_{12}H_{28}O_4Ti$ produced dye-sensitized solar with better photoelectrochemical parameters, with IPCE = 37 % at 517 nm, j= 5.53 ±0.08, V_{oc}=0.78±0.07 PCE= 4.17±0.13 FF=0.58±0.05 and less resistive to charge transport.

Acknowledgments

This study was financed in part by the Coordenação de Aperfeiçoamento de Pessoal de Nível Superior-Brasil (CAPES). The authors are also grateful to CNPq, SETI/UGF, Fundação Araucária, Finep and LABMAT-UNICENTRO for XRD measurement.

Author Contributions

Conceptualization, Gideã Taques Tractz; Bianca Vanjura Dias; Methodology, Gideã Taques Tractz; Gilherme Arielo Rodrigues Maia; Investigation, Gideã Taques Tractz; Bianca Vanjura Dias; Gilherme Arielo Rodrigues Maia.; Resources, Paulo Rogério Pinto Rodrigues; Data curation, Gideã Taques Tractz; Bianca Vanjura Dias; Guilherme Arielo Rodrigues Maia; Writing—original draft preparation, Gideã Taques Tractz; Maia.; Writing—review and editing, Gideã Taques Tractz; Bianca Vanjura Dias; Guilherme Arielo Rodrigues Maia, Paulo Rogério Pinto Rodrigues.; Supervision, Paulo Rogério Pinto Rodrigues.; Project administration, Paulo Rogério Pinto Rodrigues.; All authors have read and agreed to the published version of the manuscript.

References and Notes

[1] Smalley, R. E. *Mater. Matters* **2005**, *30*, 412. [Crossref]

[2] Chiba, Y.; Islam, A.; Watanabe, Y.; Komiya, R.; Koide, N.; Han, L. *J. Appl. Phys.* **2006**, *45*, 23. [Crossref]

[3] Kivambe, M.; Aissa, B.; Tabet, M. *Energy Procedia* **2017**, *130*, 7. [Crossref]

[4] O'Regan, B.; Grätzel, M. *Nature* **1991**, *353*, 737. [Crossref]

[5] Gratzel, M. *Nature* **2001**, *414*, 338. [Crossref]

[6] Tractz, G. T.; Maia, G. A. R.; Dias, B. V.; Ignachewski, F.; Rodrigues, P. R. P. *Quim. Nova* **2018**, *41*, 512. [Crossref]

[7] Dias, B. V.; Tractz, G. T.; Viomar, A.; Maia, G. A. R.; da Cunha, M. T.; Rodrigues, P. R. P. *J. Electron. Mater.* **2018**, *47*, 5556. [Crossref]

[8] Vitoreti, A. B. F.; Vaz, R.; Pena, A. D. L.; Raphael, E.; Ferrari, A. D. L.; Schiavon, M. A. *Rev. Virtual Quim.* **2017,** *9,* 1481 [Crossref]

[9] Guimaraes, R. R.; Parussulo, A. L. A.; Araki, K. *Electrochim. Acta* **2016**, *222*, 1378. [Crossref]

[10] Ribeiro, P. C.; da Costa, A. C. F.; Kiminami, R. H. G. A.; Sasaki, J. M.; Lira, H. L. *Mater. Res.* **2012,** *16*, 468. [Crossref]

[11] Zhang, W.; Xie, Y.; Xiong, D.; Zeng, X.; Li, Z.; Wang, M.; Cheng, Y. B.; Chen, W.; Yan, K.; Yang, S. *Mater. Interfaces* **2014**, *6*, 9698. [Crossref]

[12] Zhu, S.; Lin, S. J.; Wu, C. H.; Wu, R. J. *Sens. Actuators* **2018**, *272*, 288. [Crossref]

[13] Umale, S.; Sudhakar, V.; Sontakke, S. M.; Krishnamoorthy, K.; Pandit, A. B. *Mater. Res. Bull.* **2019**, *109*, 222 [Crossref]

[14] Dimesso, L. Handbook of Sol-Gel Science and Technology, Handbook of sol gel science and technology, 2016. [Link]

[15] Muniz, E. C.; Góes, M. S.; Silva, J. J.; Varela, J. A.; Joanni, E.; Parra, R.; Bueno, P. R. *Ceram. Int*. **2011**, 37, 1017. [Crossref]

[16] Dadkhah, M.; Salavati-Niasari, M.; Mir, N. *J. Ind. Eng. Chem.* **2014**, *20*, 4039. [Crossref]

[17] Maia, G. A. R.; Larsson, L. F. G.; Viomar, A.; Matos, L. A. C.; Antunes, S. R. M.; Maia, E. C. R.; Oliveira, M. F.; Cunha, M. T.; Rodrigues, P. R. P. *J. Mater. Sci.: Mater. Electron.* **2016**, *27*, 8271. [Crossref]

[18] X. Li, J. J.; Lenhart, H. W. Walker. *Langmuir* **2010**, *26*,

16690. [Crossref]

[19] Martínez, D.Y. T.; Pérez, R. C.; Delgado, G. T.; Angel, O. Z. *J. Mater. Sci.: Mater. Electron.* **2011**, *22*, 684. [Crossref]

[20] Guimarães, R. R.; Parussulo, A. L. A.; Toma, H. E.; Araki, K. *Electrochim. Acta* **2016**, *188*, 523. [Crossref]

[21] Larsson, L. F. G.; Tractz, G. T.; Maia, G. A. R.; Turcatel, G. J. A.; Rodrigues, P. R. P.; Cunha, M. T.; Banczek, E. D. P. *Quim. Nova* **2019**, *42*, 283. [Crossref]

[22] Hagfeldt, A.; Boschloo, G.; Sun, L.; Kloo, L.; Pettersson, H. *Chem. Rev.* **2010**, *110*, 6595. [Link]

[23] Al-Alwani, M. A. M.; Mohamad, A. B.; Ludin, N. A.; Kadhum, A. A. H.; Sopian, K. *Renewable Sustainable Energy Rev.* **2016**, *65* 183. [Crossref]

[24] Sanjay, P.; Isaivani, I.; Deepa, K.; Madhavan, J.; Senthil, S. *Mater. Lett.* **2019**, *244*,142 [Crossref]

[25] Thavasi, V.; Renugopalakrishnan, V.; Jose, R.; Ramakrishna, S. *Mater. Sci. Eng., R* **2009**, *63*, 81. [Crossref]

[26] Viomar, A.; Maia, G. A. R.I Scremin, F. R.; Khalil, N. M.; Cunha, M. T.; Antunes, A. C.; Rodrigues, P. R. P. *Rev. Virtual Quim.* **2016**, *8*, 889. [Crossref]

[27] Meen, T. H.; Jhuo, Y. T.; Chao, S. M.; Lin, N. Y.; Ji, L. W.; Tsai, J. K.; Wu, T. C.; Chen, W. R.; Water, W.; Huang, C. J. *Nanoscale Res. Lett.* **2012**, *7*, 1. [Crossref]

[28] Ako, R. T.; Peiris, D. S. U.; Ekanayake, P.; Tan, A. L.; Young, D. J.; Zheng, Z.; Chellappan, V. *Sol. Energy Mater. Sol. Cells* **2016**, *157*, 18. [Crossref]

[29] Nissfolk, J.; Fredin, K.; Hagfeldt, A.; Boschloo, G. *J. Phys. Chem. B* **2006**, *110*, 17715. [Crossref]

[30] Bisquert, J.; Fabregat-santiago, F. *J. Phys. Chem. C* **2009**, *113*, 17278.

[31] Bisquert, J.; FaVikhrenko, V. *J. Phys. Chem. C* **2004**, *108*, 2313. [Crossref]

[32] Fabregat-Santiago, F.; Bisquert, J.; Palomares, E.; Otero, L.; Kuang, D.; Zakeeruddin, S. M.; Grätzel, M. *J. Phys. Chem. C* **2007**, *111*, 6550. [Crossref]

[33] Carvalho, L. A.; Bueno, P. R. *Quim. Nova* **2006**, *29*, 796. [Crossref]

[34] Tractz, G.T.; Maia, G. A. R.; Dias, B. V.; Banczek, E. P.; Molinares, M. A.; da Cunha, M. T.; Rodrigues, P. R. P. *Orbital: Electron. J. Chem.* **2018**, *10*, 204 [Crossref]

[35] Tractz, G. T.; Maia, G. A. R.; Dias, B. V.; Banczek, E. P.; da Cunha, M.T.; Rodrigues, P. R. P. *Rev. Virtual Quim.* **2018**, *10*, 1074. [Crossref]

[36] Tractz, G. T.; Viomar, A.; Dias, B. V.; Lima, C. A.; Banczek, E. P.; Cunha, M. T.; Antunes, S. R. M.; Rodrigues, P.R.P. *J. Braz. Chem. Soc.* **2019**, *30*, 371 [Crossref]

[37] Kumara, N. T. R. N.; Ekanayake, P.; Lim, A.; Iskandar, M.; Ming, L. C. *J. Sol. Energy Eng.* **2013**, 135, 03. [Crossref]

How to cite this article

Tractz, G. T.; Dias, B. V.; Maia, G. A. R.; Rodrigues, P. R. P. *Orbital: Electron. J. Chem.* **2021**,*13*, 90. DOI: http://dx.doi.org/10.17807/orbital.v13i2.1446